Journal of Thermal Analysis and Calorimetry
https://doi.org/10.1007/s10973-024-13074-y

On optimizing the experimental setup for estimation of the thermal conductivity of thin films

V. M. Barragán[1] · E. Pastuschuk[1] · J. C. Maroto[2,3] · A. Martín[4] · S. Muñoz[1]

Received: 27 October 2023 / Accepted: 8 March 2024

Abstract
The aim of this study is to show the optimal arrangement of a measurement system for estimating the thermal conductivity of thin films from temperature profiles. For this purpose, two different experimental setup systems, with square and circular cross sections, were designed to estimate the thermal conductivity of thin films and, in particular, of two ion exchange membranes. Both systems were placed horizontally and vertically in order to evaluate the best orientation to more accurately determine thermal conductivity. A three-dimensional numerical simulation was performed using Comsol Multiphysics to predict the heat flow and temperature gradient and to evaluate the effect of the geometry and the orientation on the contact resistances. Each system was first calibrated without the membrane inside in order to estimate all the necessary thermal properties of the different materials of the model. Next, the membrane was placed inside the model, so that the model now includes the thermal conductivity of the membrane as the only unknown parameter. The numerical results were compared with the various measured temperature profiles to estimate the thermal conductivity. The thermal conductivity values of the well-known Nafion 117 membrane and other thicker membrane were determined. A very good agreement with reliable literature values was obtained. The approach presented here, combining experimental and simulated temperature profiles, may provide the basis for a practical alternative to better estimate the thermal conductivity of thin films.

Keywords Ion-exchange membranes · Thermal conductivity · Finite element Method · Contact resistance

Introduction

Nowadays, searching for energy efficient systems has aroused interest in designing thermoelectric systems with optimal thermal performance. Therefore, the thermophysical properties of each component of the system are key to achieving the best thermal performance as a goal. Nanofluids and thin films have emerged as an alternative to other conventional ones as a fundamental part in the design of various heat exchangers or non-isothermal applications respectively. Recent studies have discussed the thermal performance, efficiency and stability of thermoelectric coolers with the use of nanofluids and concluded that the solution lies in the process of surface modification [1–3]. Thin films, particularly polymeric exchange membranes, have also been shown to be key to improving thermal performance in non-isothermal applications such as fuel cells, reverse electrodialysis or electrolyzers [4].

Since temperature plays a crucial role in ensuring high performance and long-term usability of devices, a complete knowledge of the temperature distribution inside the device to predict the thermal performance of each component is essential. Therefore, an accurate estimation of the thermal conductivity is required for the overall thermal performance. This is not an easy task, especially when dealing with ion exchange membranes, due to their thickness and the clear dependence of their properties on their degree of hydration.

Therefore, the choice of a suitable method for measuring thermal conductivity and the design of a versatile

✉ S. Muñoz
smsm@ucm.es

1 Department of Structure of Matter, Thermal Physics and Electronics, Complutense University of Madrid, Madrid, Spain

2 Department of Electronics, Automation and Communications, Comillas Pontifical University, Madrid, Spain

3 Department of Science, Computing and Technology, Universidad Europea de Madrid, Madrid, Spain

4 Institute of Physical and Information Technologies (ITEFI), CSIC, Madrid, Spain

experimental setup are essential. The choice of orientation and geometry of the system can be a starting point for the design.

In previous studies, the authors validated the classical Lee's disk method [5] and temperature profiles using the finite element technique [6] as suitable methods for estimating the thermal conductivity of ion exchange membranes.

The effect of the orientation and geometry on the thermal performance focused in the natural convection has been a scientific research topic. In particular, the interest in heat dissipation in permeable materials has increased since the first empirical correlation proposed by Merkin [7] for a horizontal cylinder immersed in a porous medium or the classical problem of a rectangular cavity with different heated sidewalls [8]. Subsequently, other studies have focused on the dependence of natural convection, with air or water as working fluid, on the orientation and geometry of the heat source [9–11], with conclusions about the surface temperature or Nusselt number depending on the orientation. In particular, comparisons between horizontal and vertical sources have been made to analyze the dominant convection or conduction heat transfer during the heating or cooling process [12]. Most of these studies analyzed natural convection under steady state conditions, but unsteady natural convection flow has also been studied for rectangular and cylindrical geometries [13].

In this paper, we propose the design of two simple experimental setups, horizontal and vertical, with square and circular cross section geometries, in combination with a numerical simulation to analyze the effect of the orientation and geometry of the system. Experimental temperature profiles and a steady-state electromagnetic simulation will be used to analyze the effect of the geometry on the contact resistance. As a secondary goal, the possibility of evaluating the thermal conductivity of thin films, in particular ion exchange membranes is explored. The simulations are compared with the experimental temperature profiles. Finite element simulations have proven to be a valuable tool for the analysis of the electrochemical behavior of membranes [14], including the electro diffusion of ions [15], ionic diffusion coefficients [16], and the investigation of the role of contact resistances through the study of surface roughness effects [17]. To our knowledge, no study has used a finite element simulation to determine the thermal conductivity of ion-exchange membranes based on experimental temperature profiles for different orientations and geometries.

Materials and methods

Experimental

Membranes

Two membranes, Nafion 117 and MK40, were analyzed in this study. The polymeric ion-exchange membrane Nafion 117 supplied by DuPont de Nemours has been analyzed in this work is a non-reinforced homogeneous cation-exchange membrane consisting of a polytetrafluorethylene backbone and long fluorovinyl ether, with an equivalent mass (EW) of 1100 g eq^{-1}. There are no cross-links between the polymers.

The MK 40 membrane is a heterogeneous sulfonic polystyrene-divinylbenzene membrane prepared by incorporating a finely ground ion exchange resin into a polyethylene binder.

Membrane's thickness was measured with a PCE-THM-20 material thickness meter with a resolution of 0.0002 mm. Final value of membrane thickness was obtained by averaging the results of at least ten measurements made at different points of the sample under study. The membrane densities were determined by measuring the sample's area and mass. The results are presented in Table 1.

Experimental device

Figure 1 shows the schematics of the two devices used to obtain the experimental temperature–time profiles. The circular cross section device, hereafter referred to as CirS, consisted of two copper cylinders, with the sample to be tested positioned in the center and sandwiched symmetrically between the two cylinders. In their outer surface, the pieces had an orifice to allow the inlet and outlet flows of water at a selected temperature. With regard to the square cross section device, hereafter referred to as SqS, it consisted of seven similar copper pieces. This device has the ability to place different samples between each two pieces. In this case, a single tested sample was sandwiched

Table 1 Properties of the ion-exchange membranes used in this work

Membrane	Short name	Structure	IEC* / eq kg^{-1}	ρ^{**}/ 10^3kg m^{-3}	d^{**}/ 10^{-6} m
Nafion 117	NF 117	Homogenous non-reinforcement	0.94	1.98	186
MK-40	MK-40	Heterogeneous	2.6	1.12	450

*Specified by the manufacturer

**Measured

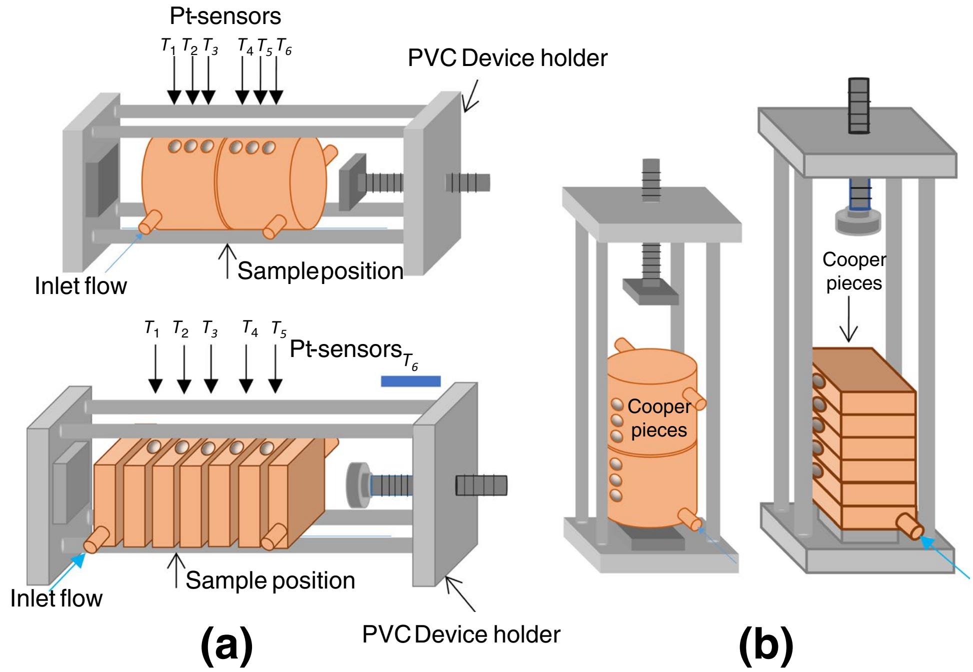

Fig. 1 Schematic of the experimental devices used. **a** Horizontal circular (top) and square (bottom) cross section devices. **b** Vertical circular (left) and square (right) cross section devices

between the third and fourth pieces. The two outer pieces had openings to allow water to flow in and out at a selected temperature. In both systems, water was circulated in only one of the metal pieces. The external surface of the other side was in contact with air at ambient temperature. In addition, a piston is placed on one side of both devices to ensure good contact between the parts and no movement in any direction. Both systems were thoroughly insulated all around to provide a one-dimensional heat flow. For the CirS device, a rubber tube insulation of 1 cm thickness was used, while for the SqS a cork board or two layers of different boards of 1 cm thickness were used for insulation.

The results confirmed this main assumption, since the heat flow was significant only along the *x*-axis.

Several holes were drilled 1 cm apart to place the temperature sensors. Pt100 sensors were placed in each hole to measure the temperature at that location.

In the CirS, the temperature was measured at six points, as shown in Fig. 1. T_1 corresponds to the value closest to the hot water inlet, and the others were numbered consecutively. Thus, sensors T_3 and T_4 correspond to the temperatures measured on both sides of the sample. The ambient temperature was measured by placing a digital thermometer around the device. In the SqS, the holes were made in the five internal parts. In this case, T_1 also corresponded to the value closest to the hot water inlet, and the rest were also numbered consecutively. The sample to be tested was then positioned between temperatures T_3 and T_4. T_6 in this case was the ambient temperature around the device. The measurements with the SqS were also made without the last part in order to try out the different possibilities and to get a better understanding of how the SqS works.

The process of achieving steady state temperatures was standardized for all measurements. The membrane sample was consistently positioned at the center. Once the water bath reached the desired temperature of 49.5 °C for CirS or 59.5 °C for SqS, it was passed through the circular orifice, and the temperature was measured for a period of 4 to 5 h. The chosen interval time was estimated beforehand to ensure steady state was reached. The flow velocity was 0.51 m s^{-1}. The first measurement was taken using the cell without the insulating cover and membrane to calibrate the model simulation.

In addition, a membrane holder was designed and characterized to be placed in the center of both systems to hold the membrane. Although the membrane sample was always dry during the study, this new system has been developed with the goal of accommodating future experimentation involving wet membranes. Both holders are easily adjustable for different membrane thicknesses. A schematic of the different membrane holders used in both devices is shown in Fig. 2. It consisted of two pieces that fit into each other, leaving a free space to place the membrane.

The material used for the membrane holder was PTFE for CirS and PLA Premium for SqS.

Finite element simulations

For our numerical simulation, we used Comsol Multiphysics® (Comsol Inc., Burlington, MA, USA), which

Fig. 2 Schematic of both membrane holders. **a** SqS device **b** CirS device. **c** A detailed cross section of the holder

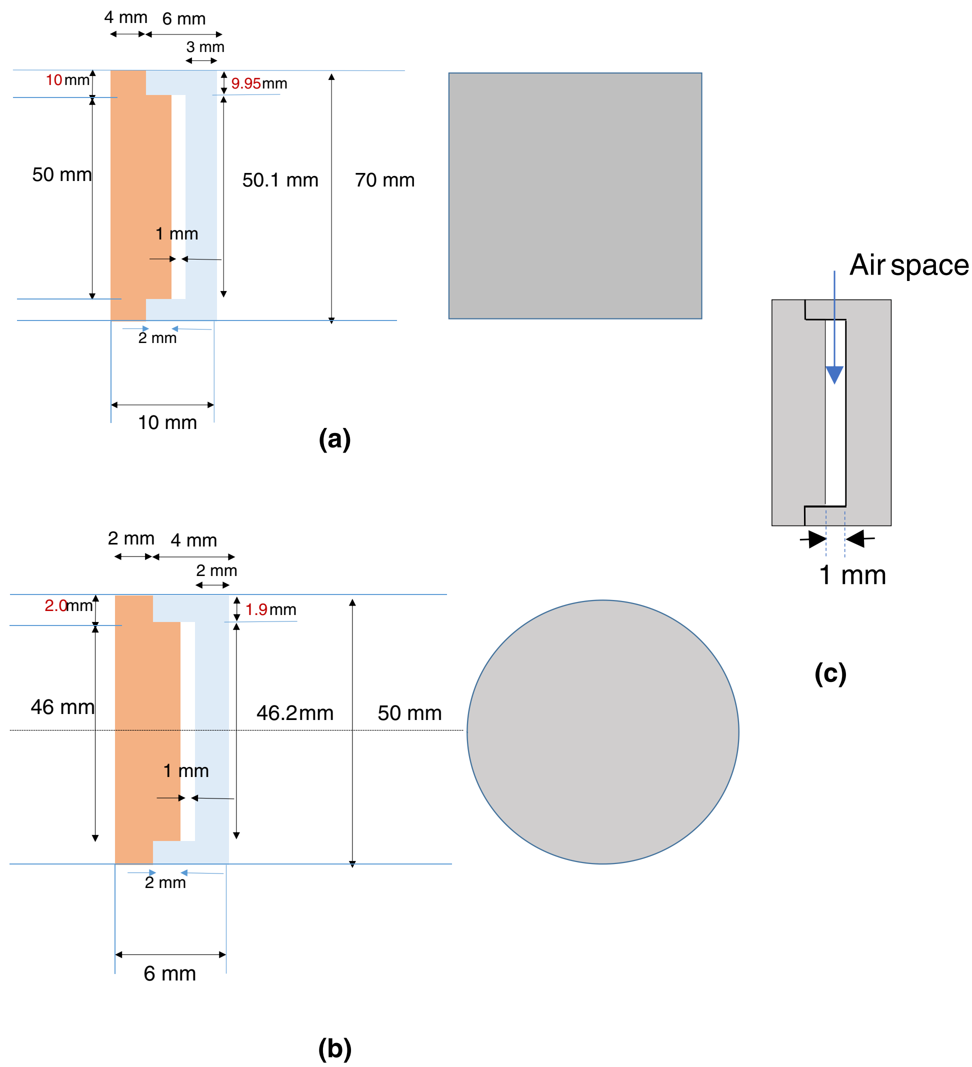

implements the FE numerical technique. In addition to the experimental systems, two other systems were designed, a square cross section with only two adjacent blocks and a circular cross section with six adjacent cylinders in addition to the two lateral ones. In this way, the effect of the orientation and the thermal contacts of both geometries can be analyzed. For this purpose, we performed a steady-state study using the Heat Transfer in Solids module to solve the differential form of the Fourier's law. In a previous study [6], the authors showed the calibration of a simple cylindrical system, placed horizontally and without insulation, by calculating the temperature profiles at the same six positions measured with the experimental setup. Thus, six temperature probes were placed inside these holes to determine the temperature values, denoted Ti, $i = 1$ to 6. In contrast to the experimental sensors, these probes can provide the minimum, maximum and average temperature value along the hole or are only located on both sides of the membrane. As for the SqS device, it was designed with seven blocks of $5 \times 5 \times 1$ cm side by side. For both systems, the water flowed through two additional hollow cylinders, perpendicular to the left of the system, with radii of 0.25 cm and thicknesses of 1.5 mm. Figure 3 depicts various geometries designed using Comsol. Three models similar to the experimental ones are displayed in (a), whereas the models shown in (b) correspond to supplementary models created exclusively for our numerical simulation.

The inlet block is modeled as a forced convection consisting of a long horizontal tube with water circulating at a velocity of 0.51 m s^{-1} at the bath temperature. In a first step, to simulate the experimental model, the temperature of the flow was the same than in the corresponding experimental case. Afterward, for all the models the temperature was set to 50 °C (denoted by Tbath in Fig. 3) in order to compare the results. All contact surfaces were set as thermal contacts to define the correlations for the conductance at the interface of two surfaces. Due to the fact that the dimensions involved in the different parts of the system vary by several orders

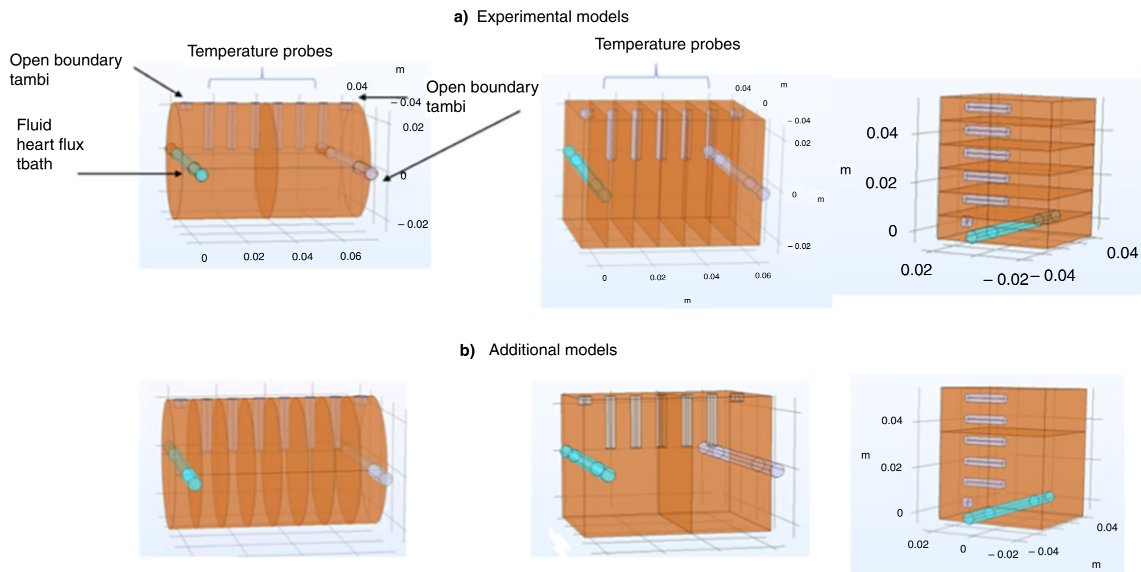

Fig. 3 Square and circular cross section models designed in Comsol

of magnitude (microns for the membrane compared to millimeters for the two external cylinders), an adaptive mesh is used so that the size of the base tetrahedron varies for the different regions. A steady-state study was performed using a parametric sweep. Unlike the measurements, the ambient temperature was set to 20 °C in the simulation to eliminate additional effects due to changes in material properties with temperature. The iterative process of fitting the calculated temperature profile to both experimental setups, determines the unknown thermal properties of the solid materials used in the experimental setup. This procedure is then repeated for the systems with the insulating shell and the membrane holder. Once the elements are characterized, simulations permit to study the influence of geometry, position, or any other interesting parameter, without the necessity of experimental data.

A summary of material properties, either calculated or specified by the manufacturer, is given in Table 2.

Once the system is characterized, the membrane is placed without a gap in the center of the model, or between the third and fourth block for systems with different blocks. The membrane sample was simulated with the same geometry as the corresponding system, either circular or square cross-section, as shown in Fig. 2. The sample was always dry. The membrane is set as a thin thermally resistive layer in the numerical modeling. As the authors have previously estimated [5, 6] the thermal conductivity of different ion-exchange membranes, we used the value obtained for Nafion 117 membrane to check the results obtained in this study. A value of 0.25 W m^{-1} K^{-1} was obtained for the thermal conductivity of a Nafion 117 membrane. We calculate it again to validate our simulation. The results show good agreement between both studies and in comparison, to other previous studies [15] that estimated values of Nafion 117 thermal conductivity around 0.2 W m^{-1} K^{-1}.

The advantages of the proposed method are twofold: first, this study may be a preliminary stage useful to ensure that our experimental design is the best choice; second, the membrane holder requires a small membrane surface and it is adjustable to any thickness. Although this study has focused on dry membranes, we would like to point out that the approach presented here may be applicable to determine the thermal properties of thin films or wet membranes thanks to the membrane holder.

Table 2 Material properties used in the numerical simulation

Material	Thermal conductivity / W m^{-1} K^{-1}	Density / kg m^{-3}
Copper	388**	8962*
Rubber shell	0.035*	29.8*
Cork 1 shell	0.041*	159
Cork 2 shell	0.058*	266*
PLA	0.13*	1240*
PTFE	0.3*	2130*
Nafion 117	*k*mem**	1980*
MK 40	*k*mem**	1120*

*Specified by the manufacturer

**Determined by comparison with experimental temperature profiles

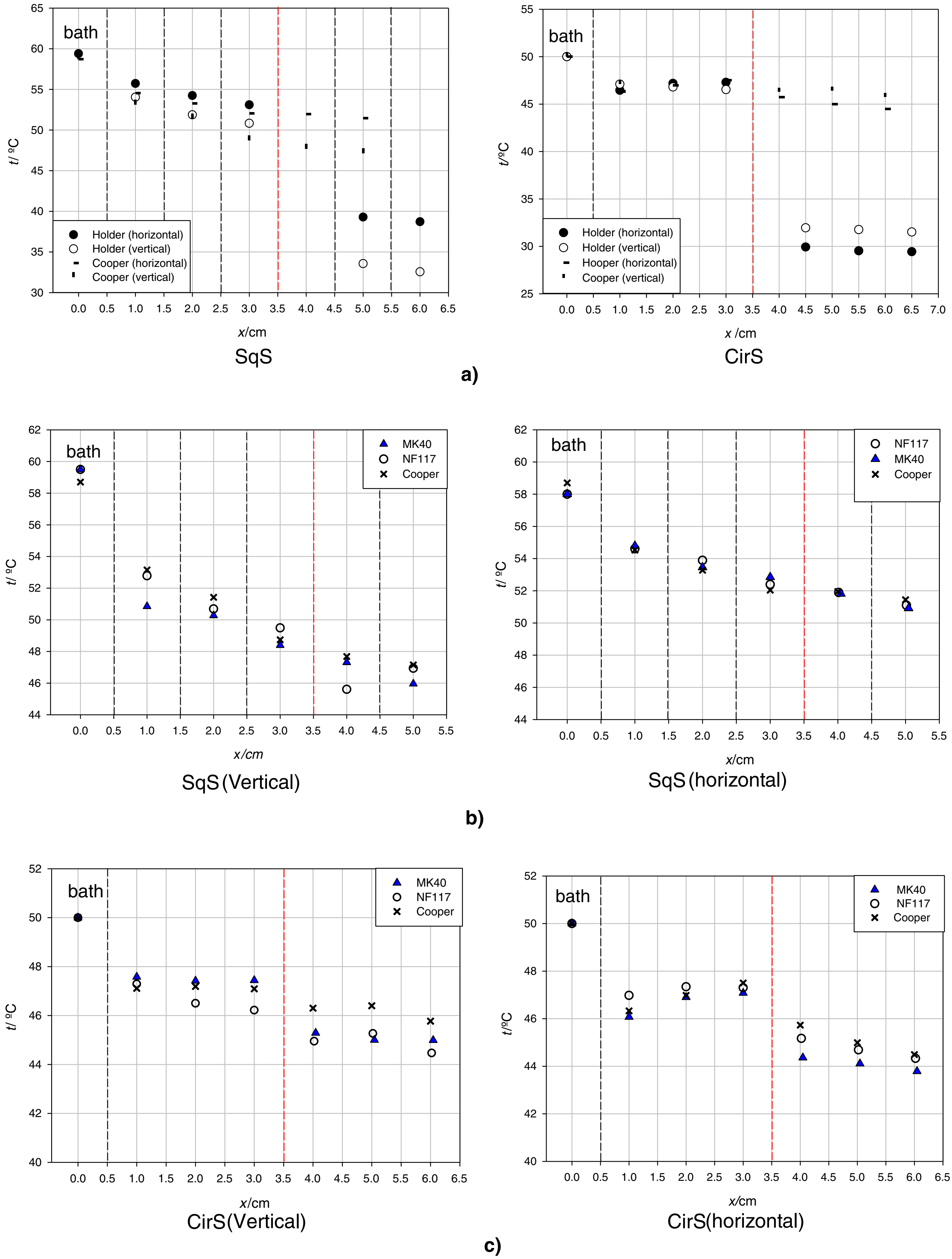
bath
Holder (horizontal)
Holder (vertical)
Cooper (horizontal)
Cooper (vertical)
t/ ºC
x/cm
SqS
bath
Holder (horizontal)
Holder (vertical)
Hooper (horizontal)
Cooper (vertical)
t/ºC
x /cm
CirS
a)
bath
MK40
NF117
Cooper
t/ ºC
x/cm
SqS (Vertical)
bath
NF117
MK40
Cooper
t/ ºC
x/cm
SqS (horizontal)
b)
bath
MK40
NF117
Cooper
t/ ºC
x/cm
CirS(Vertical)
bath
MK40
NF117
Cooper
t/ ºC
x/cm
CirS(horizontal)
c)

◂**Fig. 4** Experimental temperature profiles for the models studied. The dots represent the temperature measured in each Pt-sensor. The bath temperature is also shown to the left of each graph. **a** A comparison of results using only copper versus the membrane holder for both devices, **b** A comparison of SqS with and without membrane samples, **c** A comparison of CirS with and without the membrane samples. Red line indicates sample position

Results and discussion

Experimental temperature profiles.

Figure 4 shows the experimental temperature profiles for both systems, with and without the membrane, with membrane holder, and placed horizontally and vertically. of the orientation was higher in SqS, probably due to a higher contribution of the contact resistances between blocks in this position. As was expected the inclusion of a sample leads to a more significant temperature gradient from left to right mainly with the membrane holder, with higher thickness. Thus, a significant decrease of the temperature on the right side is observed.

As for the CirS, formed with only two blocks, this showed negligible contact resistances, as it was expected mainly when is placed vertically or with the membrane holder. Likewise, the membrane holder significantly increases the temperature gradient from left to right. Compared to the SqS, the temperature on the right side was lower for the horizontal arrangement and similar for the vertical one.

Figure 4a shows the temperature profiles found for both devices, without sample, in horizontal (Hor) and vertical (Vert) positions. We can see that the influence.

The membrane increases the temperature gradient for both systems and layouts. The presence of the membrane emphasizes the contact resistances of the SqS vertically. Likewise, the membrane seems to increase the contact resistances of the CirS although some values do not follow a perfect line or a precise pattern.

Simulated temperature profiles.

We calculated the temperature profiles for the models designed in Comsol for each parametric sweep under steady state. Figure 5a shows the comparison between the measurements with the six Pt-sensors, represented by dots, and the profiles obtained with the simulation. In the rest of the graphs in Fig. 5, this comparison is not possible because the bath temperature was different in each case and the simulation tried to make this temperature value uniform in order to compare the different systems used.

The results for the cylindrical geometry always showed lower contact resistances than the square geometry for vertical orientation, while the differences were not significant for horizontal orientation. At the beginning of the simulation, the temperature profiles of both systems without membrane sample were fitted to the experimental ones. As it is shown for the examples in Fig. 5, the agreement is generally good, although there are some values of the temperature probes showed a value discrepant from the trend expected. The presence of the membrane holder results in higher temperature gradients, which are higher for the cylindrical device when the devices are placed horizontally and vice versa when placed vertically. In addition, the contact resistance of the rectangular device is minimized.

When the membrane sample was included, both devices showed similar trends to the behavior without it. That is, the cylindrical device has the lowest contact resistances, especially to the left of the membrane, while the rectangular one still shows large differences between both configurations which would confirm again its high values of contact resistances. The temperature gradient between the two sides of the MK40 membrane was lower.

From the results, it can be concluded that the vertically placed cylindrical device would be the most reliable device for estimating the thermal conductivity of thin films so that the contact resistances are lower.

Estimation of the thermal conductivity.

In addition to the temperature profiles, we also calculated the amount of heat transferred through the membrane, denoted by Q, for the models with membrane designed in Comsol for each parametric sweep at steady state. To achieve our secondary objective of the present study, which was to calculate the thermal conductivity of the membrane, two probes were placed just on both sides of the membrane to measure the temperature and thus calculate the temperature gradient, denoted by ΔT. Both thermal parameters are related by the thermal conductivity, k as follows;

$$\Delta T = \frac{QL}{A\kappa} \tag{1}$$

Thus, the thermal conductivity is calculated, knowing the thickness, L, and the area of the membrane, A. Table 3 shows the thermal conductivity values obtained for each system studied.

As shown, the values obtained for the membrane conductivity are very similar for the cylindrical geometry in the different configurations, while the rectangular

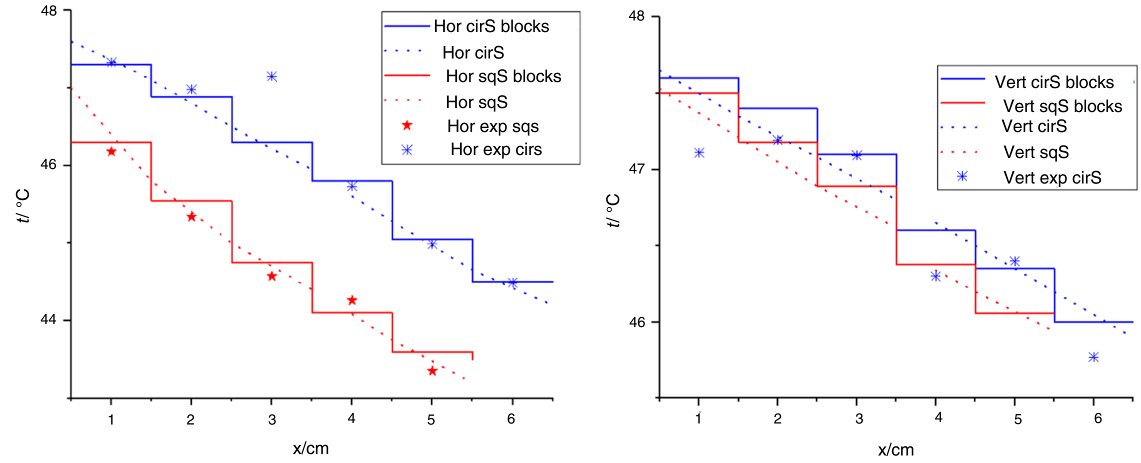
Hor cirS blocks
Hor cirS
Hor sqS blocks
Hor sqS
Hor exp sqs
Hor exp cirs
t/ °C
x/cm
Vert cirS blocks
Vert sqS blocks
Vert cirS
Vert sqS
Vert exp cirS
t/ °C
x/cm

a)

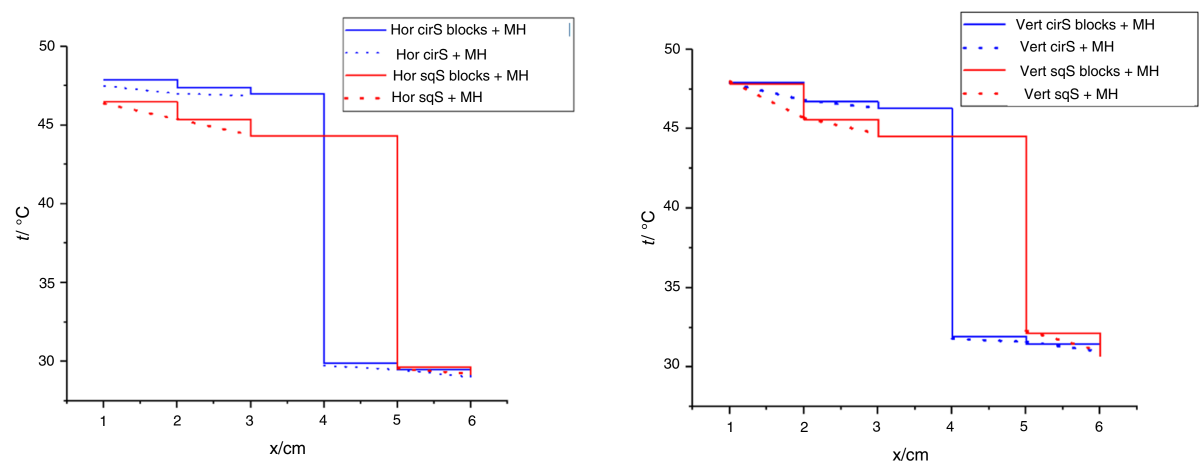
Hor cirS blocks + MH
Hor cirS + MH
Hor sqS blocks + MH
Hor sqS + MH
t/ °C
x/cm
Vert cirS blocks + MH
Vert cirS + MH
Vert sqS blocks + MH
Vert sqS + MH
t/ °C
x/cm

b)

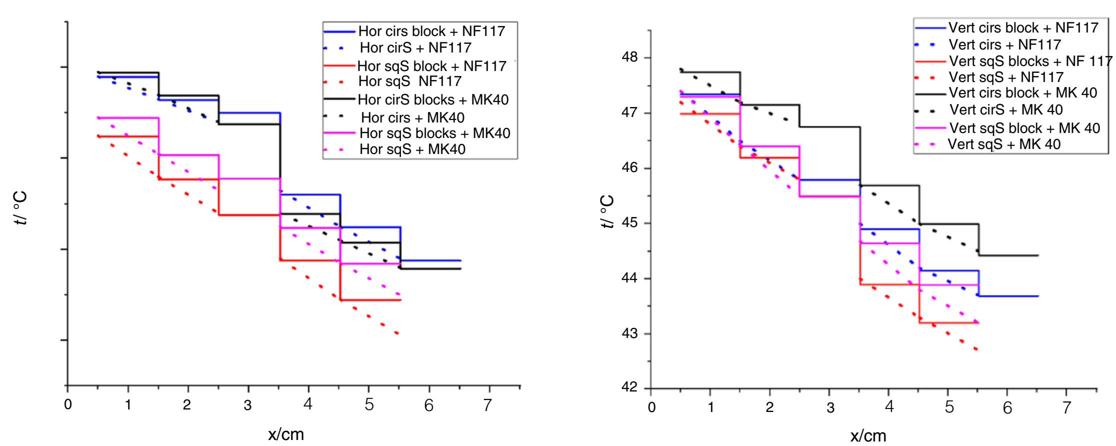
Hor cirs block + NF117
Hor cirS + NF117
Hor sqS block + NF117
Hor sqS NF117
Hor cirS blocks + MK40
Hor cirs + MK40
Hor sqS blocks + MK40
Hor sqS + MK40
t/ °C
x/cm
Vert cirs block + NF117
Vert cirs + NF117
Vert sqS blocks + NF 117
Vert sqS + NF117
Vert cirs block + MK 40
Vert cirS + MK 40
Vert sqS block + MK 40
Vert sqS + MK 40
t/ °C
x/cm

c)

◂**Fig. 5** Temperature profiles calculated, with several blocks and only with two blocks, for the models studied. **a** Only the blocks, simulated and measured values, **b** with the membrane holder (MH) and **c** with both membranes

Table 3 Estimated values for the thermal conductivity of the tested membranes

System	Thermal conductivity NF 117 / W m^{-1} K^{-1}	Thermal conductivity MK 40 / W m^{-1} K^{-1}
SqS Hor 5 blocks	0.19 ± 0.01	0.4 ± 0.01
SqS Hor 2 blocks	0.18 ± 0.01	0.39 ± 0.01
SqS Vert 5 blocks	0.22 ± 0.01	0.4 ± 0.01
SqS Vert 2 blocks	0.2 ± 0.01	0.37 ± 0.01
CirS Hor 6 blocks	0.22 ± 0.01	0.41 ± 0.01
CirS Hor 2 blocks	0.21 ± 0.01	0.42 ± 0.01
CirS Vert 6 blocks	0.25 ± 0.01	0.44 ± 0.01
CirS Vert 2 blocks	0.24 ± 0.01	0.43 ± 0.01

geometry showed higher differences and the lowest value. If the value of 0.21 W m^{-1} K^{-1} calculated for CirS in a previous study, is taken as valid for the thermal conductivity of Nafion, the values estimated for the remaining cases studied are in the range of 0.18 W m^{-1} K^{-1} to 0.25 W m^{-1} K^{-1}. The values obtained may validate this method for estimating the thermal conductivity of thin membranes, so that the values obtained are in good agreement with those reported in the literature for this well-known membrane, which varied in the interval 0.1–0.25 W m^{-1} K^{-1} depending on the method used. The results for the MK40 membrane showed less variation between the different configurations and led to similar conclusions as those for the Nafion membrane. These results may confirm that this method is adequate for evaluating contact resistances and thermal conductivity of thin films. These results again confirm that the CirS, preferably in a vertical position, may be the most reliable system for studying the thermal performance of thin films.

Conclusions

The combination of experimental and simulated temperature profiles shows to be a valid approach to gain insight into the role of geometry and orientation of the system based on the thermal performance. Both systems showed better performance when placed vertically and the circular cross section system seems to be the most reliable geometry. The results indicate the ability of the proposed setup systems to detect the thermal properties of the different materials used and provide a basis for estimating the thermal conductivity of thin films and in particular of ion exchange membranes. Thus, the thermal conductivity is determined with the only requirement that the membrane density and thickness are known. The proposed method is validated with the excellent agreement obtained for the Nafion 117 membrane in the context of reliable literature values. The model developed can provide, in addition to the thermal conductivity, other quantities of interest, such as the heat flux or the contact resistance, which can shed light on new studies for better and more efficient design of membrane-based devices with optimal temperature performance.

Acknowledgements Financial supports of this work by Banco de Santander and Universidad Complutense de Madrid within the framework of Project PR75/18-21589 and the Project for Research Groups (Bioelectromagnetism Research Group 910305) are gratefully acknowledged.

Author contributions VMB contributed to Conceptualization, Methodology, Validation, Formal Analysis, Investigation, Resources, Writing-review & editing, Visualization, Funding acquisition. EP contributed to Validation, Writing-review & editing. JCM contributed to Validation, Formal Analysis, Writing-review & editing. AM contributed to Validation, Formal Analysis, Writing-review & editing. SM contributed to Methodology, Validation, Software, Writing-original draft, Visualization, Funding acquisition.

Funding Open Access funding provided thanks to the CRUE-CSIC agreement with Springer Nature.

Declarations

Conflict of interest Disclosure of potential conflicts of interest.

References

1. Mandev E, et al. Performance analysis of thermo-electric cooling systems equipped with surface-modified and recycled nanofluids. J Enhanc Heat Transf. 2023;30(3):33–50.
2. Afshari F, et al. Experimental and numerical study on air-to-nanofluid thermoelectric cooling system using novel surface-modified Fe3O4 nanoparticles. Microfluid Nanofluidics. 2023;27(4):1–21.
3. Gülmüş B, Muratçobanoğlu B, Mandev E, Afshari F. Experimental and numerical investigation of flow and thermal characteristics of aluminum block exchanger using surface-modified

and recycled nanofluids. Int J Numer Methods Heat Fluid Flow. 2023;33(8):2685–709.

4. Ralaiarisoa M, et al. In situ investigation of ion exchange membranes reveals that ion transfer in hybrid liquid/gas electrolyzers is mediated by diffusion, not electromigration. J Mater Chem A. 2023;11(25):13570–87.
5. Barragán VM, Maroto JC, Pastuschuk E, Muñoz S. Testing a simple Lee's disc method for estimating throuh-plane thermal conductivity of polymeric ion-exchange membranes. Int J Heat Mass Transf. 2022;184:122295.
6. Barragán VM, Izquierdo-Gil MA, Maroto JC, Antoranz P, Muñoz S. Estimation of the through-plane thermal conductivity of polymeric ion-exchange membranes using finite element technique. Int J Heat Mass Transf. 2021;176:121469.
7. Merkin JH. Free convection boundary layers on axi-symmetric and two-dimensional bodies of arbitrary shape in a saturated porous medium. Int J Heat Mass Transf. 1979;22(10):1461–2.
8. Batchelor GK. Heat transfer by free convection across a closed cavity between vertical boundaries at different temperatures. Q Appl Math. 1954;12(3):209–33.
9. Rasheed SA, Hasan AJ. Effect of orientation on the natural convection heat transfer from a heated triangular prism embedded in porous media. Case Stud Therm Eng. 2022;35:102134.
10. El Ghandouri I, El Maakoul A, Saadeddine S, Meziane M. Design and numerical investigations of natural convection heat transfer of a new rippling fin shape. Appl Therm Eng. 2020;178:115670.
11. Bunjaku F, Filkoski RV. Optimisation of thermal and geometric parameters of cylindrical fins during natural convection. Energies. 2023;16(4):1997.
12. Tripathi R, R. M. K,. Experimental investigation on natural convection in cylindrical enclosure having different orientations. Saudi J Eng Technol. 2019. https://doi.org/10.21276/sjeat.2019.4.4.6.
13. Nada SA. Natural convection heat transfer in horizontal and vertical closed narrow enclosures with heated rectangular finned base plate. Int J Heat Mass Transf. 2007;50(3–4):667–79.
14. Morf WE, Pretsch E, De Rooij NF. Computer simulation of ion-selective membrane electrodes and related systems by finite-difference procedures. J Electroanal Chem. 2007;602(1):43–54.
15. Kuldeep P, Kauranen H, Pajari R. Pajarre, Murtomäki L. Electrodiffusion of ions in ion exchange membranes: Finite element simulations and experiments. Chem Eng J Adv. 2021;8:100169.
16. Kuldeep JA, Manzanares P, Kauranen S. Mousavihashemi, Murtomäki L. Determination of ionic diffusion coefficients in ion-exchange membranes: strong electrolytes and sulfates with dissociation equilibria. Chem Electro Chem. 2022;9(11):1–11.
17. Grujicic M, Zhao CL, Dusel EC. The effect of thermal contact resistance on heat management in the electronic packaging. Appl Surf Sci. 2005;246(1–3):290–302.